

Segregation by Primary Phase Factors: A Full-wave Algorithm for Model Order Reduction

Thomas J. Klemas^{*}
tklemas@alum.mit.edu

Luca Daniel^{*}
luca@mit.edu

Jacob K. White^{*}
white@mit.edu

ABSTRACT

Existing Full-wave Model Order Reduction (FMOR) approaches are based on Expanded Taylor Series Approximations (ETAS) of the oscillatory full-wave system matrix. The accuracy of such approaches hinges on the worst case interaction distances, producing accurate models over a very narrow band of frequencies. In this paper we present Segregation by Primary Phase Factors (SPPF), a novel algorithm for FMOR enabling wideband interconnect impedance analysis. SPPF extracts exponential terms (primary phase factors) and then approximates the smoother remainder with an ETAS, thus resulting in good accuracies over a very wide band of frequencies. We also present a technique to improve conditioning for the required computation. Example results are given for simple interconnect structures modeled using a discretized mixed potential integral equation formulation.

Categories and Subject Descriptors: C.4 [Performance of Systems]: Modeling techniques

General Terms: Algorithms

Keywords: Full-wave Impedance Extraction, Model Order Reduction

1. INTRODUCTION

In order to analyze and correct on-chip signal integrity problems, a general strategy is partly in-place and partly still emerging. First, an efficient model for the interconnect is extracted from the layout geometry using one of two approaches depending on required accuracy. When the accuracy requirements are modest, a complicated lumped-element approximation is generated by identifying geometric patterns and then reduced using circuit-oriented model-order reduction (MOR) [3, 2]. When more stringent accuracy is required, an efficient model is generated by using integral

equation based field solvers [4, 14] along with sparsification acceleration [10, 7, 12] and model-order reduction [15]. Once the interconnect model has been extracted, that reduced-order model (ROM) is combined with the transistor-level circuit description and analyzed using circuit simulation or with a circuit-level timing analyzer.

There are many unresolved issues associated with above basic strategy, and one of those issues is associated with the growing importance of full-wave phenomena. Full-wave phenomena is becoming more prevalent because of the ever-increasing operating frequencies and the expanded length scales in Systems on Board (SoB) and Systems on Package (SoP) problems. Although there are fast field solvers for full-wave analysis, either for the thin conductor case [13] or for full three-dimensional analysis [14, 16], the problem of extracting reduced-order models from these full-wave solvers has received less attention.

Reduced order models can be generated from full-wave analysis by first using the full-wave solver to compute tables of frequency response data, and then fitting the results using recently developed guaranteed passive techniques [1]. An alternative, and possibly more efficient, strategy was suggested in the seminal paper on extending MOR methods to fast integral-equation based full-wave analysis [11]. That method was intended for problems in which the geometry was only a couple of wavelengths, and its accuracy hinged on a Taylor series expansion which becomes too costly when the frequencies are too high and the length scales too long.

In the next sections we introduce our formulation and describe the series based method. In section 3, we present the Segmentation by Primary Phase Factors (SPPF) algorithm which can be applied in conjunction with MOR and PFFT algorithms to improve full-wave impedance analysis. In addition, we describe a technique to improve conditioning. Using SPPF-FMOR, the accuracy of the underlying truncated Taylor series approximation to the system is bounded by the SPPF parameter \tilde{R} , thereby decoupling the error from the worst-case interaction distances and allowing accuracy over a greater frequency range than previous methods [11]. Our results, in section 4, will demonstrate the dramatic improvement in model accuracy. However, as promising as the accuracy results are for rapid characterization of a model's frequency-dependent behavior, the time-domain models that are most naturally produced contain delay-differential equations with questionable stability properties. Such issues must be examined before these models can be used to accelerate time domain simulation.

^{*}T. Klemas, L. Daniel, and J. White are with the Research Laboratory for Electronics at the Massachusetts Institute of Technology: 77 Massachusetts Avenue, Cambridge MA 02139, <http://www.rle.mit.edu/cpg/>

Permission to make digital or hard copies of all or part of this work for personal or classroom use is granted without fee provided that copies are not made or distributed for profit or commercial advantage and that copies bear this notice and the full citation on the first page. To copy otherwise, to republish, to post on servers or to redistribute to lists, requires prior specific permission and/or a fee.

DAC 2005, June 13–17, 2005, Anaheim, California, USA.
Copyright 2005 ACM 1-59593-058-2/05/0006 ...\$5.00.

2. BACKGROUND

2.1 System Formulation

This paper will present results for impedance models extracted by an extended version of the FastPep [6] solver, which we modified to improve conditioning and capture full-wave effects. Our solver approximates the unknown currents and charges of a mixed surface and volume IE using piecewise constant basis functions [5], discretizes the IE with Galerkin procedures, and enforces current and voltage conservation with mesh analysis to generate a full-wave model:

$$\overbrace{M \begin{bmatrix} \frac{s}{c} \mathbf{R} + (\frac{s}{c})^2 c \mathbf{L}(s) & \mathbf{0} \\ \mathbf{0} & \frac{\mathbf{P}(s)}{c} \end{bmatrix} M^T \mathbf{I}_C = \frac{s}{c} \mathbf{V}}^{\mathbf{Z}(s)} \quad (1)$$

$$\mathbf{I}_O = \frac{s}{c} \mathbf{V}^T \mathbf{Z}(s)^{-1} \mathbf{V}$$

in which $s = i2\pi f$ is proportional to frequency f , c is the speed of light, \mathbf{M} relates loop voltages to branch voltages, \mathbf{M}^T relates branch currents from loop currents, \mathbf{R} specifies branch resistances, $\mathbf{L}(s)$ specifies the frequency dependent branch inductances, $\mathbf{P}(s)$ is the potential coefficient matrix, \mathbf{I}_C is the vector of n mesh loop currents, \mathbf{V} is the vector of source voltages, which is zero everywhere except at the source loops, and \mathbf{I}_O is the desired output current.

2.2 Model Order Reduction Background

Taylor series expansions of $\mathbf{Z}(s)$ has been used to extend traditional projection-based MOR [3, 11]. To see how, consider the Taylor series expansion of $\mathbf{Z}(s)$ about $s = s_T$:

$$\mathbf{Z}(s) \approx \mathbf{Z}_0 + \Delta \mathbf{Z}_1 + \frac{\Delta^2}{2} \mathbf{Z}_2 + \dots + \frac{\Delta^{n_T-1}}{(n_T-1)!} \mathbf{Z}_{n_T-1}, \quad (2)$$

where $\Delta = (s - s_T)$, $\mathbf{Z}_j = \frac{\partial^j \mathbf{Z}}{\partial s^j}(s_T)$, and n_T is the truncation order. Following the method in [11], the n_T -th order equation (2) can be reduced to a n_T order state space description (or n_T 1st order equations) by introducing new "current" state variables. This results in the expanded Taylor Approximation system (ETAS):

$$\begin{bmatrix} (s_T - s) \begin{bmatrix} -\mathbf{Z}_1 & -\mathbf{Z}_2 & \dots & -\mathbf{Z}_{n_T-1} \\ \frac{\mathbf{I}}{2} & \mathbf{0} & \dots & \mathbf{0} \\ \mathbf{0} & \ddots & \ddots & \mathbf{0} \\ \vdots & \mathbf{0} & \frac{\mathbf{I}}{n_T-1} & \mathbf{0} \end{bmatrix} \\ + \begin{bmatrix} \mathbf{Z}_0 & \mathbf{0} & \dots \\ \mathbf{0} & \mathbf{I} & \ddots \\ \vdots & \ddots & \ddots \end{bmatrix} \end{bmatrix} \begin{bmatrix} \mathbf{I}_{C1} \\ \mathbf{I}_{C2} \\ \vdots \\ \mathbf{I}_{Cn_T} \end{bmatrix} = \begin{bmatrix} \mathbf{V} \\ \mathbf{0} \\ \vdots \\ \mathbf{0} \end{bmatrix} \quad (3)$$

We abbreviate the ETAS (3) by introducing the script notation:

$$[\mathcal{Z}_1 - (s - s_T)\mathcal{Z}_2]\mathcal{I}_C = \mathcal{V}. \quad (4)$$

To generate a reduced order approximation to (2), consider applying projection based MOR. In projection based MOR, a matrix \mathbf{U} is created which will project the system from n -dimensional space into a q -dimensional subspace:

$$\mathbf{U} = [\mathbf{u}_1 \quad \mathbf{u}_2 \quad \dots \quad \mathbf{u}_q], \quad q \ll n. \quad (5)$$

The columns of \mathbf{U} can be selected in a variety of ways [9], we used the Krylov subspace approach as in

$$\mathbf{u}_i \in \left\{ \mathbf{Z}_1^{-1} \mathbf{v}, (\mathbf{Z}_1^{-1} \mathbf{Z}_2) \mathbf{Z}_1^{-1} \mathbf{v}, (\mathbf{Z}_1^{-1} \mathbf{Z}_2)^2 \mathbf{Z}_1^{-1} \mathbf{v}, \dots, (\mathbf{Z}_1^{-1} \mathbf{Z}_2)^q \mathbf{Z}_1^{-1} \mathbf{v} \right\} \quad | \quad \mathbf{U}^T \mathbf{U} = \mathbf{I}.$$

\mathbf{U} is carefully constructed [3] so that its span will contain or be located very close to the exact solution to the unknown n currents: $\mathcal{I}_C \approx \mathbf{U} \widehat{\mathcal{I}}_C$ where $\widehat{\mathcal{I}}_C$ is the new "reduced" state vector. Thus, the reduced system will be:

$$[\widehat{\mathcal{Z}}_1 - (s - s_T)\widehat{\mathcal{Z}}_2]\widehat{\mathcal{I}}_C = \widehat{\mathcal{V}}, \quad (6)$$

where

$$\widehat{\mathcal{V}} = \mathbf{U}^T \mathbf{v}, \quad \widehat{\mathcal{Z}}_1 = \mathbf{U}^T \mathbf{Z}_1 \mathbf{U}, \quad \widehat{\mathcal{Z}}_2 = \mathbf{U}^T \mathbf{Z}_2 \mathbf{U}. \quad (7)$$

For the full-wave case, we must approximate the model in equation (1) with the ETAS (3) in order to apply projection MOR, our "exact solution" is actually an approximate system, and we "carefully" construct \mathbf{U} to project into a subspace that is in close proximity to the exact solution of equation (4). From [3] we know the best solution in the selected q -dimensional subspace will match the first $2q$ s -parameter moments of the solution to the approximate model in (4).

3. SEGREGATION BY PRIMARY PHASE FACTORS (SPPF)

Because the accuracy of any ROM generated by the techniques described in the previous section is dependent on the ETAS, there are severe limitations using this method in the full-wave regime for many geometries of interest. The full-wave kernel present in each element of the system matrix can be expanded:

$$\frac{e^{ikr}}{r} = \frac{1}{r} \sum_{j=0}^{n_T-1} \frac{(ikr)^j}{j!} + \underbrace{\frac{1}{r} \sum_{j=n_T}^{\infty} \frac{(ikr)^j}{j!}}_{\rightarrow 0 \text{ if } n_T \gg |kr|}. \quad (8)$$

where $ik = s/c$ is the inverse wavelength when $s = i2\pi f$ and f is the excitation frequency. The high order terms in the expansion in (8) will decay rapidly when $kr \ll 1$, corresponding to low frequencies and short distances. For SoB and SoP problems, frequencies can exceed 20 GHz and lengths can be of the order of a few centimeters. For such problems, $kr > 10$, and the series expansion in (8) requires more than 29 terms to be 1% accurate. The implication is that the ETAS system in (4) would be 29 times larger than the system in (1).

3.1 Improving ETAS with SPPF

Elements of the $\mathbf{Z}(s)$ matrix in (1) approximately have the form:

$$\mathbf{Z}_{mn} = \frac{e^{-ikr_{mn}}}{r_{mn}} \quad (9)$$

where r_{mn} is interaction distance.

The idea of the SPPF method is to pick a radius \check{R} such that $k\check{R} = O(1)$ for all frequencies of interest. Then, expand each distant \mathbf{Z}_{mn} about the full-wave kernel evaluated at an

integer multiple of \check{R} , as in

$$\frac{e^{-ikr_{mn}}}{r_{mn}} = \frac{e^{-ik(\check{R}l_{mn}+d_{mn})}}{r_{mn}} \approx \frac{e^{-ik\check{R}l_{mn}}}{r_{mn}} \sum_{j=0}^{n_T} \frac{(-ikd_{mn})^j}{j!}, \quad (10)$$

where $l_{mn} = 1, \dots, \check{n}$ and d_{mn} is such that kd_{mn} is small and therefore the series expansion converges rapidly.

Thus, SPPF segregates $\mathbf{Z}(s)$ into multiple remainder phase matrices, each corresponding to a primary phase factor, and approximates the remainder terms:

$$\mathbf{Z}(s) = \sum_{l=0}^{\check{n}} e^{-ik\check{R}l} \mathbf{P}_l \check{\mathbf{Z}}(s) \approx \sum_{l=0}^{\check{n}} e^{-ik\check{R}l} \sum_{j=0}^{n_T-1} \frac{\Delta(s)^j \mathbf{P}_l \check{\mathbf{Z}}_j}{j!}, \quad (11)$$

where $[\check{\mathbf{Z}}]_{mn} = z_{mn} e^{ikd_{mn}} / r_{mn}$. The \mathbf{P}_l operators select the entries in $\check{\mathbf{Z}}$ corresponding to the l -th phase factor $e^{ikl\check{R}}$. Equation (11) can be expanded into the SPPF-ETAS:

$$\mathbf{V} \approx \check{\mathbf{Z}}(s) \check{\mathbf{J}} = \sum_{l=0}^{\check{n}} e^{-ik\check{R}l} \mathbf{P}_l \begin{bmatrix} \check{\mathbf{Z}}_0 & \mathbf{0} & \dots \\ \mathbf{0} & \mathbf{I} & \ddots \\ \vdots & \ddots & \ddots \end{bmatrix} \quad (12)$$

$$- \Delta(s) \begin{bmatrix} -\check{\mathbf{Z}}_1 & -\check{\mathbf{Z}}_2 & \dots & -\check{\mathbf{Z}}_{n_T-1} \\ \frac{\mathbf{I}}{2} & \mathbf{0} & \dots & \mathbf{0} \\ \mathbf{0} & \ddots & \ddots & \mathbf{0} \\ \vdots & \mathbf{0} & \frac{\mathbf{I}}{n_T-1} & \mathbf{0} \end{bmatrix} \begin{bmatrix} \check{\mathbf{I}}_{C1} \\ \check{\mathbf{I}}_{C2} \\ \vdots \\ \check{\mathbf{I}}_{Cn_T} \end{bmatrix},$$

or in abbreviated SPPF-ETAS form:

$$\check{\mathbf{Z}}(s) \check{\mathbf{J}} = \sum_{l=0}^{\check{n}} e^{-ik\check{R}l} \mathbf{P}_l (\check{\mathbf{Z}}_1 - (s - s_T) \check{\mathbf{Z}}_2) \check{\mathbf{I}}_{\mathbf{C}} = \mathbf{V}. \quad (13)$$

3.2 SPPF with FMOR

Full-wave MOR is readily applied to equation (13), by pre and post-multiplying the SPPF-ETAS (13) by the projection matrix \mathbf{U} to obtain a full-wave ROM:

$$\hat{\check{\mathbf{Z}}}(s) \hat{\check{\mathbf{I}}}_{\mathbf{C}} = \sum_{l=0}^{\check{n}} \mathbf{U}^T e^{-ik\check{R}l} \mathbf{P}_l (\check{\mathbf{Z}}_1 - (s - s_T) \check{\mathbf{Z}}_2) \mathbf{U} \hat{\check{\mathbf{I}}}_{\mathbf{C}}$$

$$\mathbf{u}^T \mathbf{V} = \sum_{l=0}^{\check{n}} e^{-ik\check{R}l} (\hat{\check{\mathbf{Z}}}_{1l} - (s - s_T) \hat{\check{\mathbf{Z}}}_{2l}) \hat{\check{\mathbf{I}}}_{\mathbf{C}} = \hat{\mathbf{V}} \quad (14)$$

The cost of generating (14) from (13) is nearly equal to the cost of generating (6) from (4), using ETAS-FMOR. For a given frequency of interest, the cost of evaluating $\hat{\mathbf{I}}_{\mathbf{C}}$ given $\hat{\mathbf{V}}$ in (4) is similar to the cost of the same computation using (6). Thus, the cost of SPPF-FMOR is comparable to ETAS-FMOR in [11], but the accuracy of SPPF-FMOR is much greater for a given n_T .

3.3 Improving conditioning

The ETAS (3) and SPPF-ETAS (13), required to apply projection MOR, have poor conditioning because the \mathbf{Z}_l blocks in the top row have very different magnitudes. One can see this by examining the \mathbf{Z}_l blocks in the top (block) row of equation (3): The elements of the l -th matrices have the form $r^{l-1} e^{ikr}$. Thus, the blocks \mathbf{Z}_l each have very different magnitudes, resulting in poor conditioning for the overall system. Letting $\Delta = j(k_T - k)$, we made the following

alterations to the ETAS (and SPPF-ETAS) to improve conditioning:

$$\Delta \begin{bmatrix} -\mathbf{Z}_1 & -\frac{\mathbf{Z}_2}{\beta} & \dots & -\frac{\mathbf{Z}_{n_T-1}}{\beta^{(n_T-2)}} \\ \frac{\mathbf{I}}{2} & \mathbf{0} & \dots & \mathbf{0} \\ \vdots & \ddots & \ddots & \mathbf{0} \\ \mathbf{0} & \mathbf{0} & \frac{\mathbf{I}}{n_T-1} & \mathbf{0} \end{bmatrix} \quad (15)$$

$$+ \begin{bmatrix} \mathbf{Z}_0 & \mathbf{0} & \dots & \mathbf{0} \\ \mathbf{0} & \frac{\mathbf{I}}{\beta} & \mathbf{0} & \vdots \\ \vdots & \mathbf{0} & \ddots & \mathbf{0} \\ \mathbf{0} & \dots & \mathbf{0} & \frac{\mathbf{I}}{\beta} \end{bmatrix} \begin{bmatrix} \mathbf{I}_{C1} \\ \mathbf{I}_{C2} \\ \vdots \\ \mathbf{I}_{Cn_T} \end{bmatrix} = \begin{bmatrix} \mathbf{V} \\ \mathbf{0} \\ \vdots \\ \mathbf{0} \end{bmatrix},$$

β is a representative average distance for the system. By rescaling the blocks \mathbf{Z}_l , this modification improved the condition number of the ETAS and SPPF-ETAS dramatically: Examples demonstrated an improvement of five to ten orders of magnitude!

4. RESULTS

We highlight the advantages of the SPPF-FMOR algorithm using two wires in a transmission line configuration of length=2cm, width=37e-6m, and height=15e-6m, separated by 1cm, excited by a 1 ampere amplitude current source at one end and an open circuit at the other end. Our solver discretized the transmission line into $n = 183$ unknowns. For excitation wavelengths around 2cm (15 GHz), this example is in the full wave regime.

Figure 1 shows the phase computed from the original model ($n = 183$, extracted by the solver) and phase computed by the ROMs ($q = 14$) generated by SPPF-FMOR and ETAS-FMOR. The SPPF-FMOR phase matches over the entire frequency range, but the ETAS-FMOR phase deviates after the first resonance at about 11 GHz. Both ROMs are generated from approximations that are truncated to $n_T = 6$ terms. 10 moments from the main expansion point at $s_T = 5\text{GHz}$ and 4 moment terms from an additional expansion point (multi-point MOR [3]) at about 11 GHz are included in the projection matrix \mathbf{U} .

Figure 2 compares the log of the error in the current computed by the 2 ROMs ($q = 14$). The ROM generated by SPPF-FMOR has less than 2% error over the entire frequency range up to 15 GHz, including 2 resonance points, and is 100 times more accurate than the ETAS-FMOR model.

Both ROMs have dimension $q = 14$ and were constructed from approximate models truncated to $n_T = 6$ terms, so that the cost, $O(q n_T n^2)$ operations, to generate the SPPF-FMOR model for a parameter sweep is equivalent 84 frequency point solves. Since the ETAS-FMOR model is accurate only over a fraction of the frequency range, at least 3 ROMs would be required to accurately characterize the range, which would be equivalent to 252 frequency point solves. Therefore, if many more solves are required to accurately characterize the frequency behavior of the system over a large range, SPPF-FMOR could significantly accelerate the frequency sweep by characterizing the entire range in 1 ROM.

Although SPPF-FMOR can be used to accelerate frequency sweeps, it may be more useful as a way to generate

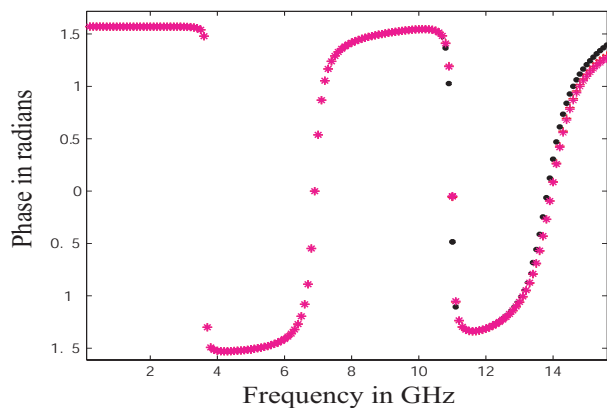


Figure 1: Phase of the Admittance computed by original model(+), SPPF-FMOR (*), and ETAS-FMOR(.). The SPPF-FMOR model matches the original over the entire frequency range up to 15GHz but the ETAS-FMOR model(.) deviates after the resonance at 11GHz.

time domain models. However, direct generation of time domain descriptions from (14) will produce delay differential equations with delays on derivatives of state variables. It is difficult to assess the stability of such systems, and their time integration also poses challenges. These issues will need to be addressed.

5. CONCLUSIONS

Segmentation by Primary Phase Factors has great potential for efficient, accurate full-wave Model Order Reduction. SPPF-FMOR models were 100 times more accurate than those generated by previous (ETAS-FMOR) methods. Our new method to rescale the ETAS blocks dramatically improved conditioning and facilitated MOR. SPPF-FMOR has been extended for PFFT sparsification [8] and to create ROMs based on multiple expansion points (multi-point MOR). Future work will involve generating passive time domain models, examining elaborate structures, analyzing cost, and constructing multi-parameter ROMs. The authors would like to acknowledge support from the Semiconductor Research Corporation, and the MARCO Interconnect Focus and Gigascale System Research Centers.

6. REFERENCES

- [1] C. P. Coelho, J. Phillips, and L. M. Silveira. A convex programming approach for generating guaranteed passive approximations to tabulated frequency-data. *IEEE Transactions CAD on Integrated Circuits and Systems*, 23(2):293–301, Feb 2004.
- [2] P. Feldmann and R. W. Freund. Efficient linear circuit analysis by Padé approximations via the Lanczos process. In *EURO-DAC'94 with EURO-VHDL'94*, September 1994.
- [3] E. Grimme. *Krylov Projection Methods for Model Reduction*. PhD thesis, Coordinated-Science Laboratory, University of Illinois at Urbana-Champaign, Urbana-Champaign, IL, 1997.
- [4] R. F. Harrington. *Field Computation by Moment Methods*. MacMillan, New York, 1968.
- [5] H. Heeb and A. E. Ruehli. Three-dimensional interconnect analysis using partial element equivalent circuits. *IEEE Trans. On Circuits and Systems I: Fundamental Theory and Applications*, 39(11):974–982, November 1992.

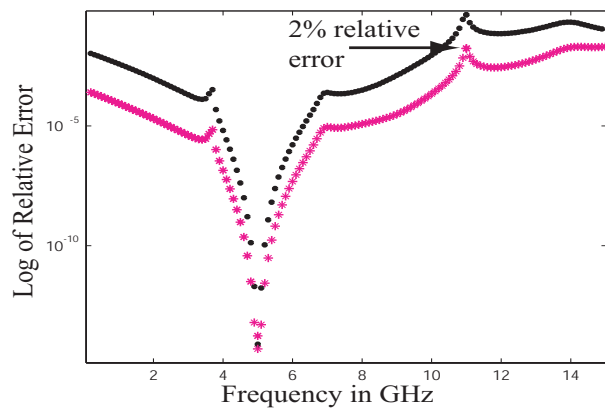


Figure 2: Log relative error of admittance computed by ROMs ($q = 14$). The relative error of SPPF-FMOR (*) is less than 2% over the entire frequency range up to 15GHz and is almost 100 times smaller than the relative error of ETAS-FMOR (.).

- [6] M. Kamon, N. Marques, and J. K. White. FastPep: a fast parasitic extraction program for complex three-dimensional geometries. In *Proc. of the IEEE/ACM International Conference on Computer-Aided Design*, pages 456–460, San Jose, CA, Nov. 1997.
- [7] S. Kapur and D. E. Long. Ies3: efficient electrostatic and electromagnetic simulation. *Computational Science and Engineering, IEEE*, 5(4):60–67, Oct-Dec 1998.
- [8] T. J. Klemas, L. Daniel, and J. White. A fast full-wave algorithm to generate low order electromagnetic scattering models. In *Proceedings IEEE APS-URSI Symposium*. IEEE Antennas and Propagation Society/URSI, July 2005.
- [9] K. Willcox and J. Peraire. Balanced model reduction via the proper orthogonal decomposition. *AIAA Journal*, 40(11):2323–2330, November 2002.
- [10] K. Nabors and J. K. White. FastCap: a multipole accelerated 3-d capacitance extraction program. *IEEE Trans. on Computer-Aided Design of Integrated Circuits and Systems*, 10(11):1447–59, Nov. 1991.
- [11] J. R. Phillips, E. Chiprout, and D. D. Ling. Efficient full-wave electromagnetic analysis via model-order reduction of fast integral transforms. In *Proceedings 33rd Design Automation Conference*, Las Vegas, Nevada, June 1996.
- [12] J. R. Phillips and J. K. White. A Precorrected-FFT method for electrostatic analysis of complicated 3-D structures. *IEEE Trans. on Computer-Aided Design of Integrated Circuits and Systems*, 16(10):1059–1072, Oct. 1997.
- [13] J. C. Rautio and R. F. Harrington. An electromagnetic time-harmonic analysis of shielded microstrip circuit. *IEEE Trans. Microwave Theory Tech.*, MTT-35:726–730, 1987.
- [14] A. E. Ruehli. Equivalent Circuit Models for Three-Dimensional Multiconductor Systems. *IEEE Transactions on Microwave Theory and Techniques*, MTT-22(3):216–221, March 1974.
- [15] L. M. Silveira, M. Kamon, and J. K. White. Direct computation of reduced-order models for circuit simulation of 3-d interconnect structures. In *Proceedings of the 3rd Topical Meeting on Electrical Performance of Electronic Packaging*, pages 254–248, Monterey, California, November 1994.
- [16] Z. Zhu, J. Huang, B. Song, and J. K. White. Algorithms in fastimp: a fast and wideband impedance extraction program for complicated 3-d geometries. In *Proc. of the IEEE/ACM Design Automation Conference*, Los Angeles, CA, June 2003.